MMA Memo 169: Atmospheric Coherence Times at Chajnantor

M.A. Holdaway
National Radio Astronomy Observatory
949 N. Cherry Ave.
Tucson, AZ 85721-0655
email: mholdawa@nrao.edu

April 21, 1997

Abstract

We investigate the distribution of atmospheric coherence times for long baselines and the fraction of time a given baseline will be phase stable during the months of best phase stability. The coherence times set a lower limit to the time over which the MMA electronics must allow stable integration. It is probable that radiometric phase compensation will further increase the requirements on the MMA electronics. The best quartile coherence time (at 90% sensitivity) at 100 GHz is about 4 minutes, while best quartile coherence time at 650 GHz is only 8 s.

1 Introduction

Phase errors on long time scales can be calibrated out, but phase errors on short time scales result in loss of coherence or decorrelation (Lay, 1997). Baseline based phase fluctuations of rms σ_ϕ radians will result in decorrelation of magnitude $e^{-\sigma_\phi^2/2}$ (Thompson, Moran and Swenson, 1986). The main effects of the decorrelation are loss of sensitivity and errors in imaging. The effects of decorrelation on imaging can largely be corrected if the rms phase errors are not too much larger than a radian (Holdaway and Owen, 1995), but lost sensitivity cannot be recovered. For this reason, several groups have invested great effort to remove the phase errors radiometrically prior to correlation.

The two main sources of decorrelating phase errors are the atmospheric phase fluctuations and the electronics, notably the LO. We should design the LO and electronics such that it is significantly more phase stable than the atmosphere during good conditions. This memo converts the phase monitor data taken with the 300 m site testing interferometer into estimates of the distribution of the coherence time at 100, 230, 345, and 650 GHz. If the coherence time is longer than the baseline crossing time, that baseline will be phase stable for long periods of time. We also present the fraction of time which certain baseline lengths are phase stable.

2 Coherence Times

For every 600 s block of site testing interferometer data, we calculate the temporal phase structure function and fit a power law to the short time scale part (Holdaway, Radford, Owen, and Foster, 1995). On time scales long compared to the crossing time of the interferometer, the rms phase essentially saturates. The spatial (and temporal) structure functions should flatten for baselines (or time scales) longer than the size scale of the turbulent layer, but we see no evidence for such a flattening out to 300 m. Hence, we assume that our simple one part power law describes the phase errors, and we also extrapolate beyond the $\sim$30 s crossing time when necessary. If the phase structure function does flatten out, this will not

ν [GHz]	50% t_c [s]	75% t_c [s]
100	66	228
230	16	53
345	8	25
650	2.5	8

Table 1: Median and 75% coherence times for four fiducial frequencies. Since the daytime phase stability is almost always worse than the night time phase stability, the 75% coherence times are approximately equal to the median night time coherence time.

change any of the coherence times which are less than ~30 s, but will increase some of the coherence times which are longer than ~30 s.

The temporal root structure function of the interferometer phase is fit by

$$\left(\langle(\phi(t_\circ) - \phi(t_\circ + t))^2\rangle\right)^{1/2} = \sqrt{2} a_t t^\alpha, \tag{1}$$

where $\phi(t)$ is the *interferometer* phase at some time t, and a and α are the amplitude and power law exponent of the temporal phase structure function. The factor of $\sqrt{2}$ enters because we are differencing two interferometer phases measured at two different times. Then the root temporal phase structure function (ie, the rms phase which one would expect on a long baseline on some time scale t) is

$$\sigma_\phi(t) = a_t t^\alpha. \tag{2}$$

For long baselines, the time scale over which the rms phase errors exceed some value $\sigma_\circ$, or the coherence time, is given by

$$t_c = (\sigma_\circ / a_t)^{1/\alpha}. \tag{3}$$

In this case, a "long baseline" is one for which the atmospheric crossing time is long compared to the coherence time. For each observing frequency considered, we scale the phase structure function with frequency non-dispersively. However, Hill and Clifford's (1981) calculations indicate that the water vapor is moderately dispersive in the submillimeter. For example, at 345 GHz, the wet delay is expected to be about 8% larger than the wet delay at 10 or 100 GHz. At 490 GHz, the delay will be about 20% larger than at 100 GHz. While this dispersion is a moderate effect in our coherence time estimates, the dispersion could be a major effect when extrapolating the phase from low frequencies to high frequencies.

What value should we use for $\sigma_\circ$? Since different applications may have different coherence requirements, we look at a range of $\sigma_\circ$: 11.5° results in 0.98 sensitivity, 26.3° results in 0.90 sensitivity, and 67.5° results in 0.50 sensitivity. In this study, we do not address the phase contributions from the motion of the antenna structure or the electronics, but look only at the atmosphere. Coherence time will also be a strong function of frequency, so we calculate coherence times at 100, 230, 345, and 650 GHz. The cumulative distributions of coherence times for these different circumstances are shown in Figures 1-2 for the winter months (May, June, and July, the months of best phase stability) at Chajnantor. The median and 75% coherence times for 90% sensitivity are shown in Table 1. The 75% coherence time (the coherence time is this long or longer for the 25% best conditions) will be approximately equal to the night time median coherence time as the daytime conditions are almost always worse than the night time conditions. For the millimeter frequencies, the coherence times are reasonably large, typically about a minute or longer. However, in the submillimeter, the coherence times become very short, even at the 75% level (25 s at 345 GHz and 8 s at 650 GHz). This indicates that submillimeter observations will be done only during the really good conditions (ie, the winter nights), and even then, fast switching with ~10 s cycle times will be pushed very hard.

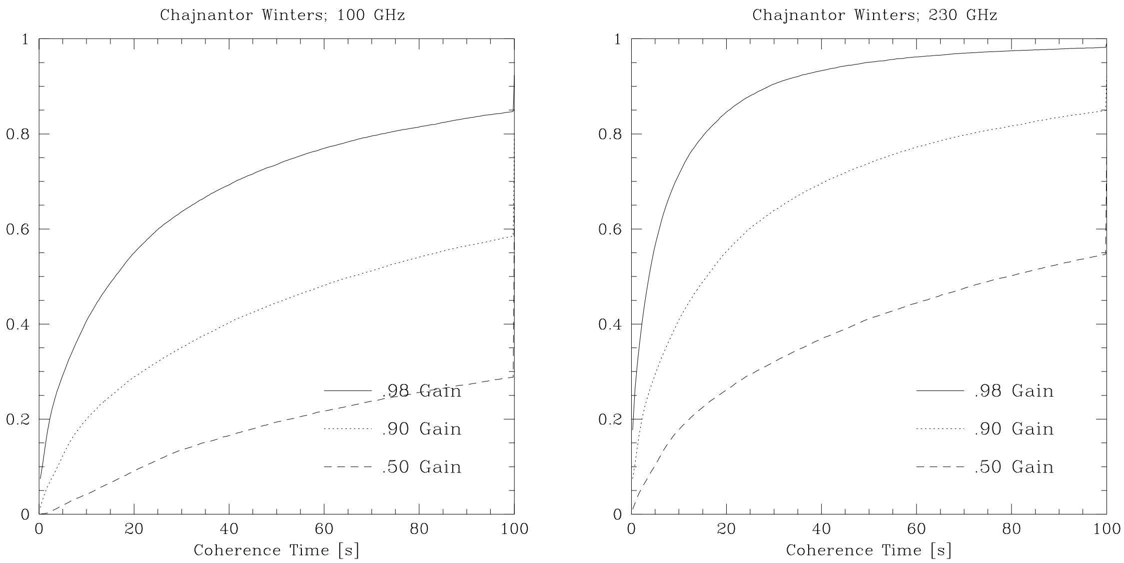

Figure 1: Cumulative distribution function of atmospheric coherence time for 98%, 90%, and 50% gain for Chajnantor during the winter season at 100 GHz and 230 GHz.

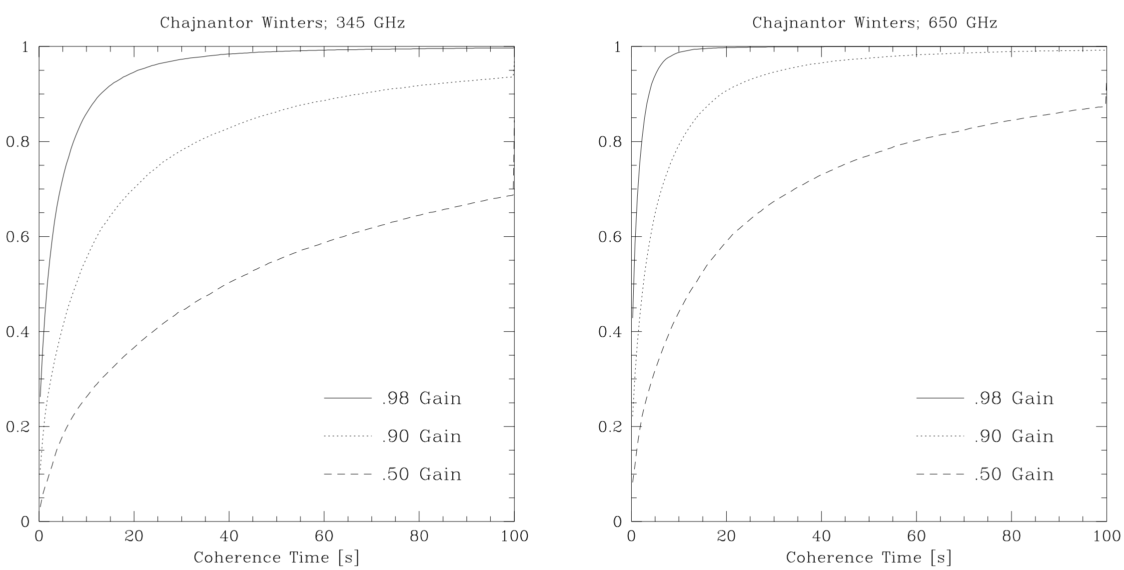

Figure 2: Cumulative distribution function of atmospheric coherence time for 98%, 90%, and 50% gain for Chajnantor during the winter season at 345 GHz and 650 GHz.

3 Maximum Coherent Baselines

The above analysis is for baselines with atmospheric crossing times which are longer than the coherence time, and does not apply to shorter baselines. The root spatial phase structure function is defined as

$$\left(\langle(\phi(\rho_\circ) - \phi(\rho_\circ + \rho))^2\rangle\right)^{1/2} = a\rho^\alpha, \tag{4}$$

where ρ is the distance between antennas and the exponent α is the same for the spatial and temporal structure functions. A short baseline will be said to be "phase stable" when

$$\sigma_\circ > a\rho^\alpha. \tag{5}$$

In this case, arbitrarily long integrations can be made (practically, this is tens of minutes). Table 2 shows the fraction of time selected baselines and frequencies will be phase stable during the winter months.

4 Radiometric Phase Compensation

The investigation of radiometric phase compensation is still ongoing, so it is not yet possible to quantify the improvements to the coherence time. However, it is expected that radiometric compensation will permit significantly increased integrations.

References

Holdaway, M.A., and Owen, F.N., 1995, "Correcting for Decorrelation Due to Atmospheric Phase Errors, MMA Memo 136.

Holdaway, M.A., Radford, Simon J.E., Owen, F.N., and Foster, Scott M., 1995, "Data Processing for the Site Test Interferometers", MMA Memo 127.

Lay, O.P., 1997, "Phase Calibration and Water Vapor Radiometry for Millimeter-Wave Arrays", *accepted to* A&A.

Thompson, Moran, and Swenson, 1986, *Interferometry and Synthesis in Radio Astronomy*, John Wiley & Sons, New York.

ν [GHz]	BL [m]	98% Gain	90% Gain	50% Gain
100	25	0.88	0.97	1.00
100	50	0.80	0.94	1.00
100	100	0.69	0.89	0.99
100	200	0.54	0.80	0.96
100	400	0.37	0.69	0.91
100	800	0.22	0.54	0.83
100	1600	0.12	0.39	0.72
230	25	0.69	0.88	0.97
230	50	0.54	0.80	0.95
230	100	0.36	0.69	0.90
230	200	0.19	0.54	0.83
230	400	0.08	0.37	0.72
230	800	0.03	0.22	0.58
230	1600	0.01	0.12	0.43
345	25	0.54	0.80	0.94
345	50	0.36	0.69	0.90
345	100	0.18	0.54	0.83
345	200	0.07	0.37	0.73
345	400	0.02	0.21	0.59
345	800	0.00	0.10	0.43
345	1600	0.00	0.04	0.28
650	25	0.25	0.62	0.86
650	50	0.09	0.44	0.78
650	100	0.02	0.26	0.66
650	200	0.00	0.12	0.50
650	400	0.00	0.04	0.33
650	800	0.00	0.01	0.19
650	1600	0.00	0.00	0.09
850	25	0.12	0.51	0.81
850	50	0.03	0.32	0.71
850	100	0.00	0.15	0.56
850	200	0.00	0.05	0.38
850	400	0.00	0.01	0.22
850	800	0.00	0.00	0.11
850	1600	0.00	0.00	0.05

Table 2: What fraction of the time is a given baseline phase stable at various frequencies?